Synchronized activity in prefrontal cortex during anticipation of visuomotor processing

Hualou Liang, Steven L. Bressler,[1,CA] Mingzhou Ding,[1] Wilson A. Truccolo[2] and Richard Nakamura[3]

[1]University of Texas at Houston, Houston, TX 77030; Center for Complex Systems and Brain Sciences, Florida Atlantic University, 777 Glades RoadBoca Raton, FL 33431; [2]Department of Neuroscience, Brown University, Providence, RI 02912; [3]Laboratory of Neuropsychology, National Institute of Mental Health, Bethesda, MD 20892, USA

[CA]Corresponding Author: bressler@fau.edu

Received 3 July 2002; accepted 28 August 2002

It is commonly presumed, though not well established, that the prefrontal cortex exerts top-down control of sensory processing. One aspect of this control is thought to be a facilitation of sensory pathways in anticipation of such processing. To investigate the possible involvement of prefrontal cortex in anticipatory top-down control, we studied the statistical relations between prefrontal activity, recorded while a macaque monkey waited for presentation of a visual stimulus, and subsequent sensory and motor events. Local field potentials were simultaneously recorded from prefrontal, motor, occipital and temporal cortical sites in the left cerebral hemisphere. Spectral power and coherence analysis revealed that during stimulus anticipation three of five prefrontal sites participated in a coherent oscillatory network synchronized in the β-frequency range. Pre-stimulus network power and coherence were highly correlated with the amplitude and latency of early visual evoked potential components in visual cortical areas, and with response time. The results suggest that synchronized oscillatory networks in prefrontal cortex are involved in top-down anticipatory mechanisms that facilitate subsequent sensory processing in visual cortex. They further imply that stronger top-down control leads to larger and faster sensory responses, and a subsequently faster motor response. *NeuroReport* 13:2011–2015 © 2002 Lippincott Williams & Wilkins.

Key words: Anticipation; Event-related potential; Local field potential; Oscillation; Response time; Prefrontal cortex; Synchronization; Top-down control

INTRODUCTION

The prefrontal cortex has been implicated in a wide range of executive functions, including top-down control over the selection and coordination of processing in sensory cortical areas [1–4]. It has been proposed that one aspect of top-down control is the imposition of facilitatory influences on sensory areas in anticipation of stimulus appearance in order to promote fast and efficient stimulus processing leading to fast and accurate responses [5–8].

The question of anticipatory top-down control by the prefrontal cortex in humans has been investigated using PET [9], fMRI [10,11] and scalp-recorded averaged event-related potentials (ERPs) [12]. Our study approached this problem through the analysis of local field potentials (LFPs) in a macaque monkey. LFPs were simultaneously recorded from chronically implanted electrodes in prefrontal and visual cortical areas as the monkey performed a visual pattern discrimination task [13]. We sought to test the hypothesis that synchronized LFP oscillations in prefrontal cortex play a role in anticipatory processes [14]. To do this, we first established the existence of a synchronized oscillatory network in prefrontal cortex as the animal was anticipating visual stimulus presentation. We then examined the statistical relations of these pre-stimulus prefrontal LFP oscillations with subsequent stimulus-evoked events in visual cortical areas during early stimulus processing, and with the motor response that ensued.

MATERIALS AND METHODS

Experiments were performed in the NIMH Laboratory of Neuropsychology. Animal care was in accordance with institutional guidelines at the time. Surgical procedures were previously described [15]. Surface-to-depth event-related LFPs were simultaneously recorded from 14 bipolar teflon-coated platinum electrodes (five dorsolateral prefrontal, one motor, two striate, two prestriate, four temporal) chronically implanted in the left cerebral hemisphere (Fig. 1a) of a highly trained macaque monkey performing a visuomotor pattern discrimination task. The data were analog filtered (−6 dB at 1 and 100 Hz, 6 dB/octave falloff) and digitized at 200 samples/s.

The monkey initiated each trial by depressing a lever with the right hand. Data collection began about 115 ms prior to stimulus onset and continued until 500 ms post-stimulus. Each stimulus consisted of four dots arranged as a (left- or right-slanted) line or diamond on a display screen. The monkey indicated whether the stimulus was a line or

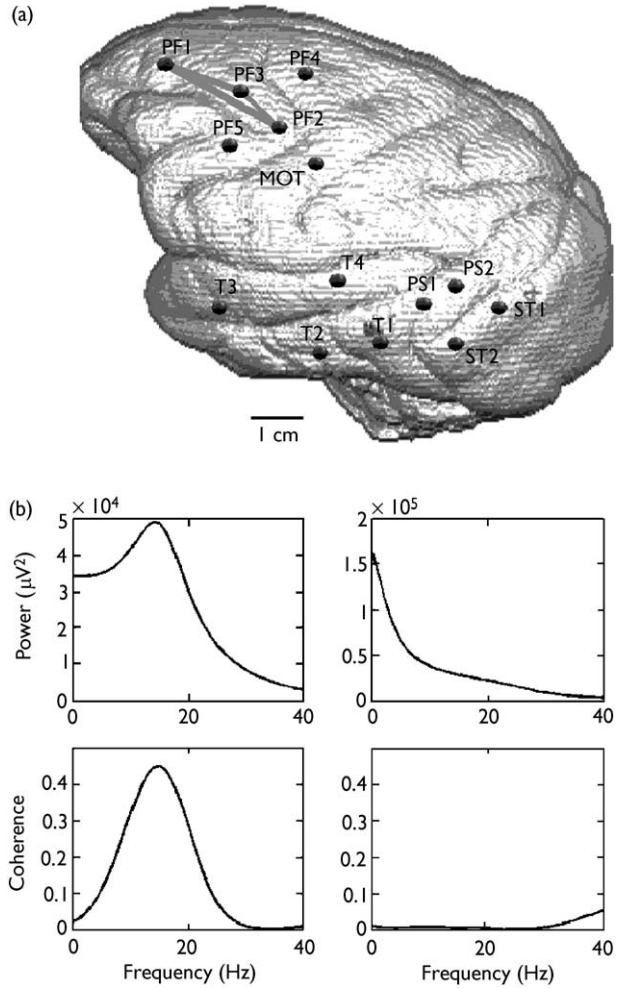

Fig. 1. Dorsolateral prefrontal network organization in the pre-stimulus period. (**a**) Approximate recording sites are marked by disks, and the pairs of sites having significant ($p < 0.01$) peak coherence are connected by lines. Display is a lateral view of the cortical surface reconstructed from magnetic resonance images of a representative rhesus macaque brain. Recording sites were estimated from maps made during surgery and from post-mortem examination of surface penetration marks. (**b**) left column: Examples of pre-stimulus network power (top) and coherence (bottom) spectra for the fastest response time group. Right column: Comparable examples of non-network power (top) and coherence (bottom) spectra.

diamond pattern by a go (lever release) or no-go (pressure maintenance) response. Because each dot position was used as part of both the line and diamond patterns, no single dot in any pattern could be used to determine whether that pattern was a line or diamond. On go trials, the monkey received a water reward at 500 ms post-stimulus if the hand was lifted before that time. On no-go trials, the lever was depressed for 500 ms post-stimulus, and released thereafter. go and no-go trials were presented with equal probability in 1000-trial sessions. Only go trials were used in this study, in a combined data set of 2052 trials recorded over eight sessions.

Correct go trials were rank ordered by response time and then sorted into groups of 200, starting with the fastest response times and proceeding to the slowest, each group sharing 50 trials with the previous one. A total of 38 groups resulted. The average response time and the averaged ERP (AERP) for each striate, prestriate and temporal site were obtained from each group. The peak amplitude and latency were identified for the two earliest AERP components.

Multivariate autoregressive (MVAR) spectral analysis was performed on the LFPs from the ensemble of trials in each group [16] during the pre-stimulus period. Specifically, spectral power and coherence were derived from a MVAR time series model fit to the LFPs in a 70 ms window starting 60 ms before stimulus onset. A bootstrap resampling procedure was employed in which power and coherence spectra were derived from MVAR models for 100 resamples of each group trial ensemble [16]. All sites and site pairs were tested to determine whether they consistently displayed power and coherence spectral peaks in the low β-frequency range over the set of bootstrap resamples, and whether the values of low β-frequency power and coherence were significantly greater than zero ($p < 0.01$). Detection of a

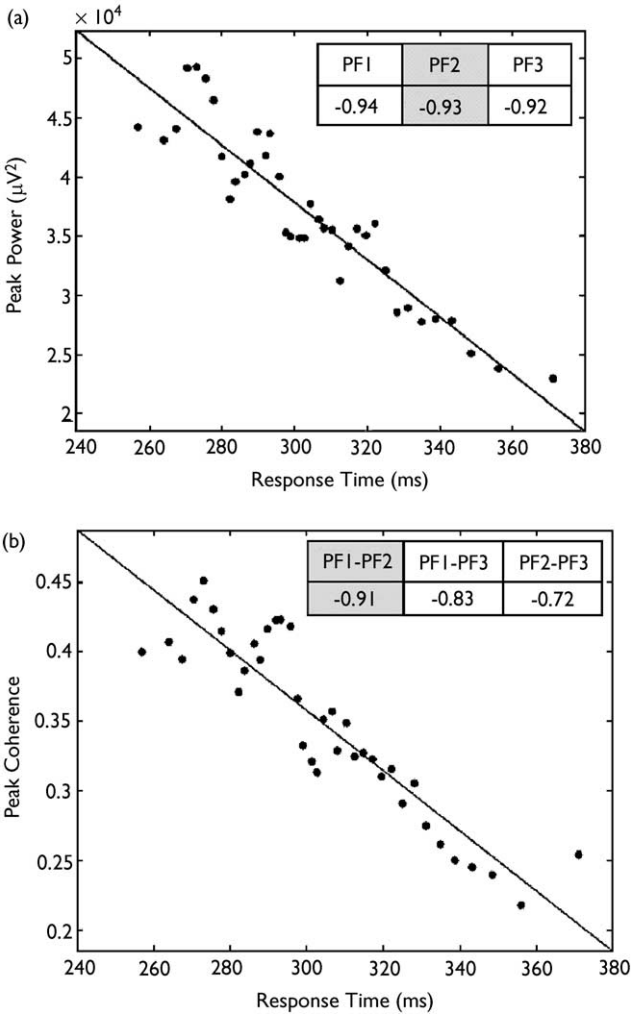

Fig. 2. Scatter plots showing strong correlation of pre-stimulus prefrontal network power (**a**) and coherence (**b**) with response time. Insets: Spearman rank correlation coefficients for all network sites (a) and site pairs (b), with plotted relations shaded. Linear least-squares best fits to the data are superimposed.

coherent oscillatory network in the prefrontal cortex was based on identifying sites having power and coherence spectral peaks that were consistently in the low β-range by bootstrapping, and also had significant peak values. The time course of the pre-stimulus oscillatory activity was analyzed using an adaptive moving window approach [16].

Spearman rank correlation coefficients were computed for the relations of (pre-stimulus) power and coherence peak values with (post-stimulus) AERP peak amplitudes and latencies, and with average response times. Use of the non-parametric Spearman rank correlation coefficient was indicated because the underlying variables were not normally distributed.

RESULTS

In the pre-stimulus interval, three of the five prefrontal sites had power spectral peaks (Fig. 1b, top left) in the low β-frequency range (mean 15.0 ± 0.9 Hz). The coherence spectra between these sites also had peaks in the same range (16.6 ± 4.4 Hz; Fig. 1b, bottom left). The power and coherence peaks of this select group of prefrontal sites implied that they participated in a synchronized prefrontal network established prior to stimulus presentation. The synchronized oscillations continued until the approximate onset of early visual stimulus processing (~90 ms after stimulus onset), at which time they underwent a rapid decline in strength. Power spectra of the other two prefrontal sites were maximal near 0 Hz and declined with increasing frequency (Fig. 1b, top right), and their coherence spectra were uniformly low (Fig. 1b, bottom right). Since these other two sites were not significantly coherent with the three network sites, they were considered not to participate in the network. Likewise, no other recorded sites outside of prefrontal cortex were significantly coherent with the network sites.

Prefrontal network strength (peak power and coherence) predicted the ensuing response time over the 38 response time groups: both pre-stimulus network power and coherence had highly significant ($p < 0.001$) correlations with response time (Fig. 2) for all network sites and site pairs (Fig. 2, insets). Peak power of the fastest response time group exceeded that of the slowest by $222 \pm 10\%$, and peak coherence by $171 \pm 32\%$. We next determined the latency and absolute value of amplitude for the first two observable AERP components of seven striate, prestriate and temporal sites. (Site T4 was excluded because it lacked a well-developed AERP.) The first component (C1) was a wave that peaked between 75 and 95 ms; the second component (C2) peaked between 100 and 140 ms (Table 1). The polarity of C1 was positive, and that of C2 was negative, at five of the seven sites. (These polarities were reversed at sites ST1 and T3, possibly due to the positioning of the bipolar electrodes with respect to the cortical lamination.)

Pre-stimulus network power and coherence were highly correlated with the amplitude and latency of the C1 and/or C2 components at select sites (Fig. 3). The results for the C1 and C2 components differed greatly as to which striate, prestriate and temporal sites showed significant correlations. Pre-stimulus power and coherence were significantly correlated ($p < 0.002$) with C1 peak amplitude at only one striate (ST1) and one prestriate (PS2) site (Table 2),

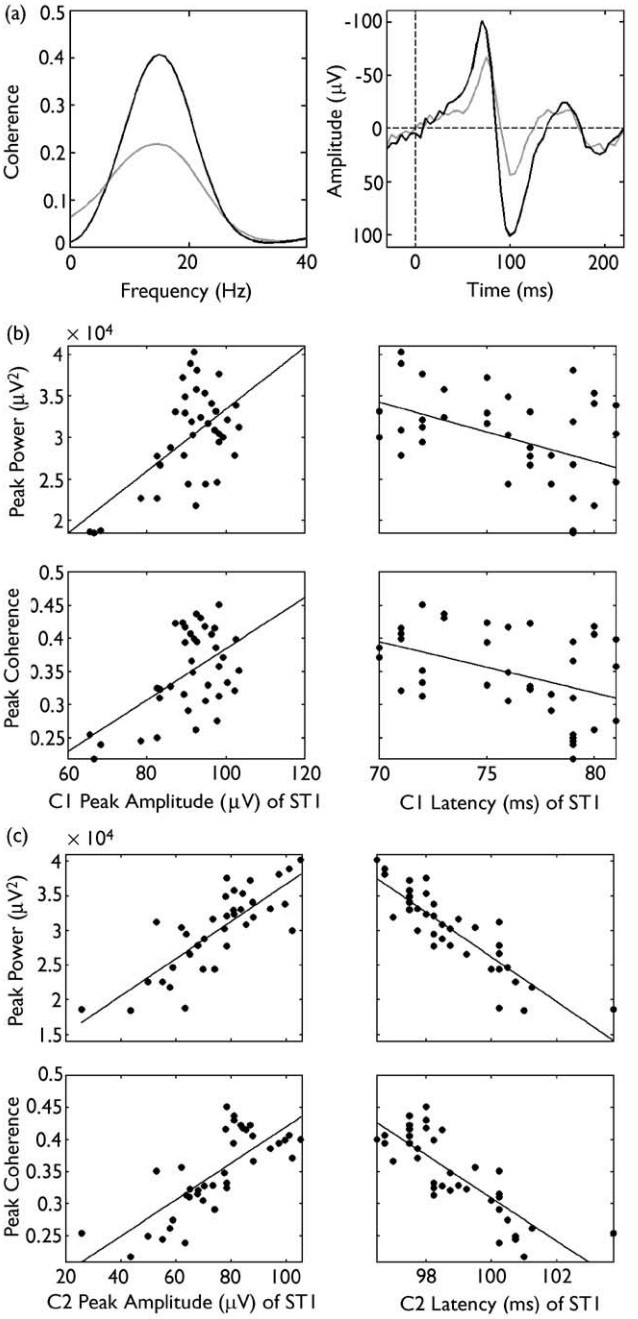

Fig. 3. Pre-stimulus prefrontal network strength (levels of peak power and coherence) and post-stimulus visual AERP varied as a function of response time. (**a**) left: As an example, the peak coherence between prefrontal sites PFI and PF2 was greater for the fastest response time group (black) than for the slowest group (gray). Right: As another example, the AERP at striate site STI showed larger early post-stimulus components for the fastest response time group (black) than for the slowest group (gray). (**b**) Scatter plots show the correlations between pre-stimulus prefrontal network strength (levels of peak power and coherence) and post-stimulus CI AERP component amplitude and latency over all 38 response time groups. Pre-stimulus prefrontal peak power at site PFI (top), and coherence between sites PFI and PF2 (bottom), were both correlated with the amplitude (left) and latency (right) of the CI AERP component. (**c**) Pre-stimulus prefrontal peak power at site PFI (top), and coherence between sites PFI and PF2 (bottom), were also both correlated with the amplitude (left) and latency (right) of the C2 AERP component.

Table 1. Mean (± s.d.) C1 and C2 peak latencies (ms) and of striate, prestriate and temporal sites

	ST1	ST2	PS1	PS2	T1	T2	T3
C1	75 ± 3.5	–	80 ± 2.3	95 ± 4.2	85 ± 2.8	90 ± 3.3	80 ± 4.4
C2	100 ± 1.6	105 ± 4.3	125 ± 2.2	135 ± 1.3	125 ± 2.2	125 ± 1.7	140 ± 2.4

– not present.

Table 2. Mean (± s.d.) Spearman rank correlation coefficient values comparing pre-stimulus prefrontal network power and coherence with the amplitude and latency of the C1 AERP component at striate, prestriate and temporal sites.

	C1 Amplitude		C1 Latency	
	Network power	Network coherence	Network power	Network coherence
ST1	0.55 ± 0.05*	0.62 ± 0.08*	−0.45 ± 0.04	−0.45 ± 0.08
ST2	–	–	–	–
PS1	0.15 ± 0.06	0.15 ± 0.08	−0.29 ± 0.03	−0.31 ± 0.07
PS2	0.72 ± 0.04*	0.53 ± 0.15*	0.02 ± 0.04	0.07 ± 0.09
T1	0.30 ± 0.05	0.31 ± 0.08	−0.22 ± 0.05	−0.16 ± 0.11
T2	0.06 ± 0.05	0.02 ± 0.15	−0.49 ± 0.03	−0.44 ± 0.07
T3	0.15 ± 0.06	0.03 ± 0.13	0.16 ± 0.03	0.17 ± 0.05

*$p < 0.002$; – not present.

Table 3. Mean (± s.d.) Spearman rank correlation coefficient values comparing pre-stimulus prefrontal network power and coherence with the amplitude and latency of the C2 AERP component at striate, prestriate and temporal sites.

	C2 Amplitude		C2 Latency	
	Network power	Network coherence	Network power	Network coherence
ST1	0.83 ± 0.05*	0.73 ± 0.10*	−0.83 ± 0.04*	−0.71 ± 0.14*
ST2	0.88 ± 0.01*	0.80 ± 0.09*	−0.79 ± 0.02*	−0.69 ± 0.08*
PS1	0.86 ± 0.05*	0.82 ± 0.04*	−0.84 ± 0.05*	−0.78 ± 0.06*
PS2	0.37 ± 0.02	0.43 ± 0.01	0.47 ± 0.05	0.38 ± 0.09
T1	0.83 ± 0.01*	0.79 ± 0.07*	−0.75 ± 0.04*	−0.68 ± 0.06*
T2	0.87 ± 0.01*	0.81 ± 0.06*	−0.83 ± 0.04*	−0.78 ± 0.03*
T3	0.76 ± 0.04*	0.62 ± 0.15*	0.28 ± 0.07	0.15 ± 0.16

*$p < 0.002$.

suggesting that these two sites were selectively influenced by anticipatory processes. The further observation that the C1 amplitude at ST1 was significantly correlated ($p < 0.01$) with that at PS2, and not at the other prestriate and temporal sites, implied, more specifically, that it was the interrelation of these two sites that was preferentially influenced. By contrast, pre-stimulus network power and coherence were significantly correlated ($p < 0.002$) with C2 peak amplitude at all seven of the striate, prestriate and temporal sites except PS2 (Table 3). Likewise, C2 amplitude at ST1 was significantly correlated ($p < 0.01$) with C2 amplitudes at prestriate site PS1 and temporal sites T1 and T2, but not at PS2. This suggested that the locus of facilitation shifted and became more widespread in the transition from the C1 to C2 components.

DISCUSSION

This study implicates synchronized oscillations in the β-frequency range within the monkey dorsolateral prefrontal cortex in mechanisms of top-down anticipatory control. The synchronization of a group of prefrontal sites was observed by detecting significant β-frequency peaks in the spectral power and coherence of prefrontal LFPs as the monkey awaited stimulus presentation. Previous studies in monkeys and cats have reported β-frequency oscillations in motor, somatosensory, and posterior parietal areas under similar conditions of focused attention and immobility [17,18]. Studies in humans have shown correlations of pre-stimulus EEG power in the δ, θ and α-frequency ranges with early AERP components [19–21], and of pre-stimulus δ and α EEG power with response time [21,22].

We expand upon these earlier findings by demonstrating that: (1) a select portion of prefrontal cortex displays synchronized oscillations in the low β-frequency range during visual stimulus anticipation; (2) the strength of synchronization predicts the amplitude and timing of early visual stimulus processing components and response timing; and (3) the visual cortical sites which show AERP components that are correlated with prefrontal pre-stimulus synchronization change in going from C1 to C2 components, suggesting that top-down facilitation may be spatially and temporally modulated [23]. Several studies have demonstrated the existence of anatomical connections between dorsolateral prefrontal areas and areas of prelunate and inferotemporal visual cortex [24–27]. These prefrontal and posterior areas include the electrode sites examined in this study, and their connections could provide a structural basis for the proposed top-down facilitatory effects.

Since the prefrontal β-oscillations essentially disappeared at approximately the time of early stimulus processing (~90 ms after stimulus onset), we conclude that they were specifically related to the stimulus anticipation, and not to other factors such as lever depression or reward expectation, both of which continued well past this time. Although our results are consistent with the idea that synchronized networks in prefrontal cortex provide top-down facilitation of visual cortical areas in anticipation of stimulus processing, we cannot rule out the possibility that one or more other brain areas coordinate the activity of both prefrontal and visual cortex.

CONCLUSION

Neuronal synchronization has been proposed as a mechanism by which a neuronal population in one area may increase the effective synaptic gain it exerts on target neurons in another area [28]. Furthermore, it has been suggested that the synchronization of β oscillations in the motor cortex may increase the efficiency of descending control exerted by corticospinal neurons on spinal motoneurons during sustained motor output [29]. Our study suggests that, analogously, the synchronized β oscillations of neurons in prefrontal cortex may increase the efficiency of their top-down control of target neurons in visual cortical areas during sustained visual anticipation.

REFERENCES

1. Teuber HL. The riddle of frontal lobe function in man. In: Warren JM and Akert YL (eds). *The Frontal Granular Cortex and Behavior.* New York: McGraw-Hill; 1978, pp. 410–444.
2. Fuster JM. *Exp Brain Res* **133**, 66–70 (2000).
3. Skinner JE and Yingling CD. Central gating mechanisms that regulate event-related potentials and behavior. In: Desmedt J (ed). *Attention, Voluntary Contraction and Event-related Cerebral Potentials.* Basel: Karger; 1977, pp. 30–69.
4. Miller EK. *Nature Rev Neurosci* **1**, 59–65 (2000).
5. Frith C and Dolan RJ. *Philos Trans R Soc Lond B Biol Sci* **352**, 1221–1230 (1997).
6. Desimone R. *Philos Trans R Soc Lond B Biol Sci* **353**, 1245–1255 (1998).
7. Duncan J. *Philos Trans R Soc Lond B Biol Sci* **353**, 1307–1317 (1998).
8. Driver J and Frith C. *Nature Rev Neurosci* **1**, 147–148 (2000).
9. Shulman GL, Corbetta M, Buckner RL *et al. Cerebr Cort* **7**, 193–206 (1997).
10. Kastner S, Pinsk MA, Weed PD *et al. Neuron* **22**, 751–761 (1999).
11. Hopfinger JB, Buonovore MH and Mangun GR. *Nature Neurosci* **3**, 284–291 (2000).
12. Hopf JM and Mangun GR. *Clin Neurophysiol* **111**, 1241–1257 (2000).
13. Bressler SL. *Brain Res Rev* **20**, 288–304 (1995).
14. Engel AK, Fries P and Singer W. *Nature Rev Neurosci* **10**, 704–716 (2001).
15. Bressler SL, Coppola R and Nakamura R. *Nature* **366**, 153–156 (1993).
16. Ding M, Bressler SL, Yang W *et al. Biol Cybern* **83**, 35–45 (2000).
17. Rougeul A, Bouyer JJ, Dedet L *et al. Electroencephalogr Clin Neurophysiol* **46**, 310–319 (1979).
18. Bouyer JJ, Montaron MF and Rougeul A. *Electroencephalogr Clin Neurophysiol* **51**, 244–252 (1981).
19. Brandt ME. *Int J Psychophysiol* **26**, 285–298 (1997).
20. Basar E, Rahn E, Demiralp T *et al. Electroencephalogr Clin Neurophysiol* **108**, 101–109 (1998).
21. Winterer G, Ziller M, Dorn H *et al. Clin Neurophysiol* **110**, 1193–1203 (1999).
22. Haig AR and Gordon E. *Psychophysiology* **35**, 591–595 (1998).
23. Martinez A, DiRusso F, Anllo-Vento L *et al. Vis Res* **41**, 1437–1457 (2001).
24. Webster MJ, Bachevalier J and Ungerleider LG. *Cerebr Cortex* **4**, 470–483 (1994).
25. Stanton GB, Bruce CJ and Goldberg ME. *J Comp Neurol* **353**, 291–305 (1995).
26. Schall JD, Morel A, King DJ *et al. J Neurosci* **15**, 4464–4487 (1995).
27. Pandya DN and Yeterian EH. *Philos Trans R Soc Lond B Biol Sci* **351**, 1423–1432 (1996).
28. Fries P, Reynolds JH, Rorie AE *et al. Science* **291**, 1560–1563 (2001).
29. Baker SN, Kilner JM, Pinches EM *et al. Exp Brain Res* **128**, 109–117 (1999).

Acknowledgements: We thank R. Coppola for recording software, G. Johnson and C. Anderson for magnetic resonance images, and T. Holroyd for surface reconstruction software. Computing facilities provided by the Charles E. Schmidt College of Science at FAU. Supported by NSF grant IBN0090717, NIMH grants MH58190 and MH42900, and ONR grant N00014-99-1.